MODE I FRACTURE OF THIN-PLY CARBON-EPOXY LAMINATES: EFFECTS OF PLY THICKNESS

Guillaume Frossard[1], Joël Cugnoni[1], Thomas Gmür[1] and John Botsis[1]

[1]Faculté des sciences et techniques de l'ingénieur, Ecole Polytechnique Fédérale de Lausanne (EPFL)
Bâtiment ME, Station 9, CH-1015 Lausanne, Switzerland
Email: john.botsis@epfl.ch, web page: http://lmaf.epfl.ch

Keywords: Thin-ply composites, Delamination, R-curve, Fibre bridging

ABSTRACT

The resistance to delamination of unidirectional fibre reinforced laminates increases with crack growth due to large scale bridging. This toughening mechanism, which is reflected by the increasing resistance curves, is subject to size effects. In this work, the influence of the ply thickness on the energy release rate (ERR) in mode I delamination of unidirectional carbon-epoxy laminates is characterized. Three ply thicknesses are considered from thin-ply (0.030 g/m^2) to thick-ply (0.150 g/m^2). While the ERR at onset of crack propagation do not depend on the ply thickness, the plateau level varies considerably. This effect is attributed to the change of homogeneity of the microstructure, which affects the amount of bridging fibres. Due to the tow spreading procedure used during the production of the prepregs, resin rich regions are present in thick ply laminates, while the fibre distribution is more homogeneous in thin-ply laminates. The heterogeneity of the microstructure increases the probability to have bundles of fibres trapped between the crack faces and eventually leads to higher bridging energy and higher ERR plateau.

1 INTRODUCTION

Thin-ply carbon-epoxy laminates have quickly gained in interest in recent years. They are produced down to approximately 20 micrometres of ply thickness by a tow spreading procedure. Thin-ply laminates offer several advantages in addition to the possibility to produce thinner and lighter structures. The first benefit is the extended design space. At a constant laminate thickness, more ply orientations can be selected. This is particularly important in thin shells, where optimized quasi-isotropic laminates may replace a basic [0°,90°,0°] cross-ply laminate [1].

The second advantage is that thin-ply laminates have higher strength properties than traditional composites. Amacher et al. [1] and Sihn et al. [2] show that the onset of damage and ultimate tensile strength of quasi-isotropic laminates are increased with decreasing ply thickness. This improvement is attributed to the change of failure mode. Progressive accumulation of damage such as transverse cracking and delamination leads the thick ply laminates to failure while thin-ply laminates exhibit a brittle failure mode [1,3].

The improvement in terms of strength is usually accompanied with lower toughness. Therefore, in order to allow a damage tolerant design approach, it is necessary to characterize and understand the ply thickness effect on the energy release rate. This study focuses on mode I interlaminar crack propagation, also called delamination because it is one of the main weaknesses of laminated composites.

In fibrous composites such as carbon-epoxy, the resistance to fracture under mode I loading increases with crack propagation before reaching a plateau. This phenomenon which is depicted in the resistance (R-) curves is attributed to fibre bridging: intact fibres bridge both crack faces. It acts as closing pressure on the crack faces following a traction-separation distribution which needs to be identified. As shown by Farmand-Ashtiani et al. [4] and Manshadi et al. [5], the R-curve is no longer a material property in case of large scale bridging. In particular it depends on the thickness of the specimen. It is therefore mandatory to understand how the crack propagation depends on scaling parameters such as the ply thickness and the specimen thickness [6].

The objective of this study is two-field: firstly the effect of the ply thickness on the mode I ERR at crack initiation and subsequent growth is characterized; secondly, the reasons of the ply thickness effect are explained thanks to mechanistic investigations.

2 MATERIALS ANS METHODS

2.1 Materials and specimen instrumentation

The material considered throughout this study is a carbon-epoxy laminate produced by North-TPT Switzerland. The unidirectional prepregs of M40JB carbon fibres and ThinPreg™ 80EP/CF epoxy with different fibre areal weights (30, 75 and 150 g/m^2) are generated from the same resin and fibre batches. Unidirectional plates are stacked by hand lay-up and cured in autoclave following the recommended curing cycle (8h30 at 80°C, vacuum and 3 bars of peak pressure). The number of layers is increased proportionally to the inverse of the ply thickness in order to keep the fibre volume fraction equal to 57±1%. These volume fractions are computed based on the thickness of the plates and the total weight of fibres. In order to guaranty a good planarity and thickness, the plates are cured between two rigid aluminium plates separated by precisely machined spacers. A 60 mm long and 20 µm thick Teflon-PTFE insert is introduced in the mid-plane of each plate as delamination initiator.

The plates are then cut to 25 mm wide beams with a diamond saw. One edge is painted white and marked every 1 mm for the crack length optical monitoring (Figure 1). The load is applied through two loading blocks glued on top and bottom surfaces of the specimen with a two-component epoxy. Table 1 summarizes the dimensions of the specimens.

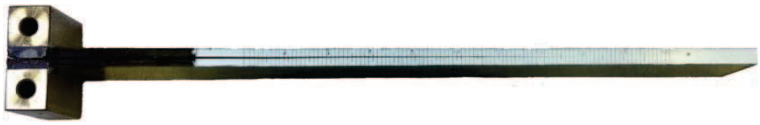

Figure 1 : Tested DCB specimen

Nominal specimen's thickness [mm]	Ply thickness [mm]	Plies / specimen [-]	Length [mm]	Width [mm]	Number of specimens [-]
3.9	0.030	130	180	25	6
3.9	0.075	52	180	25	5
3.9	0.150	26	180	25	5

Table 1 : Dimensions of the specimens

2.2 Fracture tests and data reduction

The DCB specimens are tested according to the ASTM standard [7] under displacement control at a constant rate of 2.4 mm/min. The tests are performed on an Instron® machine equipped with a 2 kN load cell. Pictures of the edge of the specimens are recorded with a high resolution CCD camera at a frequency of 1 Hz for the monitoring of the crack length.

The linearity of the behaviour of the specimen is verified by numerical model analysis and by inspection of the experimental unloading data. As a consequence, the compliance calibration method can be used to calculate the ERR associated with the crack growth:

$$G = \frac{P^2}{2b}\frac{dC}{da} \tag{1}$$

where P is the load, b the width of the specimen, C the compliance of the specimen and a the crack length. The compliance, which is the ratio between the measured applied displacement and load, is fitted by a power law $C = Ba^n$, so that the differentiation dC/da can be done analytically.

2.3 Mechanistic investigations

Cross sections observations under optical microscope are used to understand the reason of the ply

thickness effect. Embedding resin is poured in the wake of the kept open specimen in order to keep in-place the bridging zone and its fibres. Using a diamond wire saw, cross sections are then cut every 2.5 mm from the crack tip to the end of the bridging zone (Figure 2). The cross sections are embedded in resin and polished using grinding SiC papers until a grain size of grit 4000. The cross section observations under the microscope provide information about the homogeneity of the microstructure and about the number and development of bridging fibres and bundles.

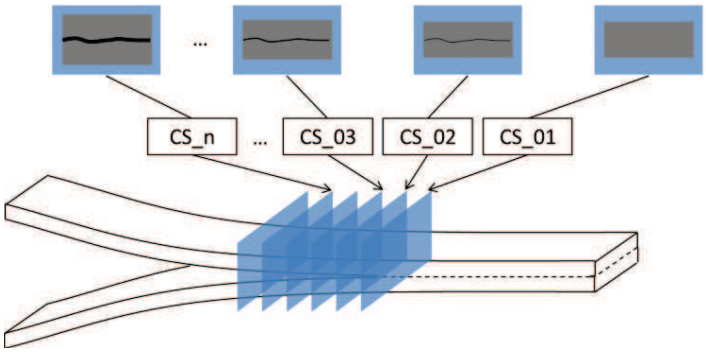

Figure 2 : Schematic of the specimen and cross sections

For each cross section, microscopic images are taken at 10x of magnification. The sequence of images is then assembled with the commercial software Photoshop in order to obtain the entire section. The crack profile is isolated using a semi-automatic tool of Photoshop called lasso magnetic. Then, the bridging fibres are identified by the use of thresholds. The number of bridging fibres is computed as the total fibre area divided by the area of a unique fibre.

The microstructure is inspected on cross sections situated close to the crack tip. The heterogeneity is quantified by calculating the coarseness, which is the standard deviation of the local fibre volume fraction $v_{f,local}$ normalized with the overall fibre volume fraction (equation (2)). By the use of an appropriate threshold, the picture is converted to a binary image so that the ratio between matrix pixels and fibre pixels can be computed. The local volume fraction is computed on 100 000 randomly distributed windows on each of the cross sections. As the coarseness is sensitive to the size of the windows, it is computed for square windows with size changing from 3 to 10 fibre diameters.

$$C = \frac{std\left(v_{f,local}\right)}{average\left(v_{f,local}\right)} \tag{2}$$

3 RESULTS AND DISCUSSIONS

3.1 Experimental results

The average R-curves with standard deviation for three series of tests are shown in Figure 3 (a). For all of them the ERR at crack initiation is nearly identical ($G_{I,i}$ =162 ± 18 J/m^2). However, the ERR at subsequent crack growth is highly increased with ply thickness. In particular the ERR at steady-state varies linearly with the ply thickness (Figure 3 (b)). The scaling independent ERR values at initiation suggest that fibre bridging is the main mechanism responsible for the scaling effects on the plateau level. It is checked that the specimen thickness does not influence the conclusions and observations concerning the ply thickness effect.

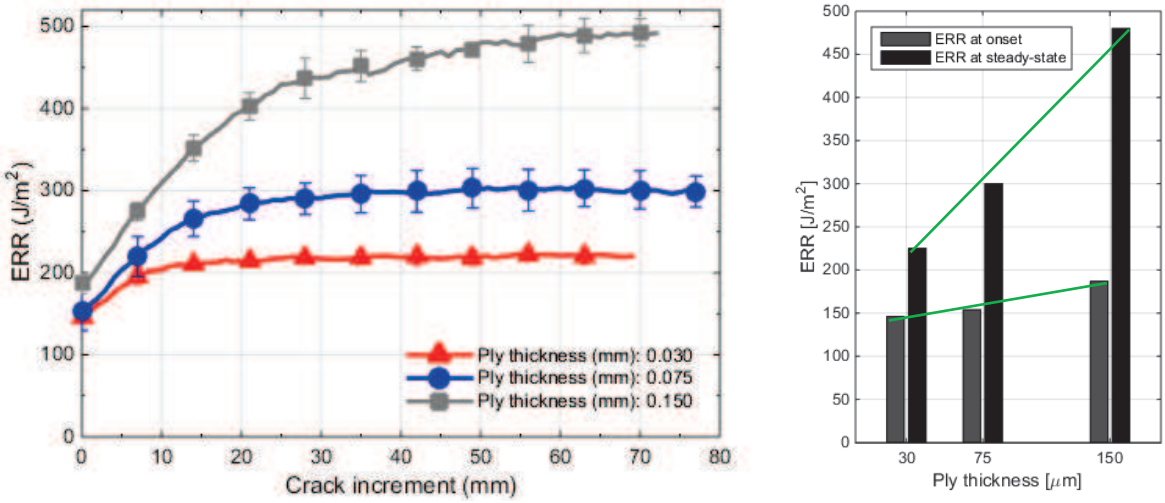

(a) (b)

Figure 3 : (a) Average R-curves obtained for the laminates of different ply thicknesses (b) Average onset and steady-state ERR for the different DCB tests

3.2 Phenomenological explanation of the ply thickness effect

As the ply thickness does not affect the mechanical properties of the laminate, its effect on the steady-state ERR must be explained by differences in the microstructure. Figure 4 shows cross sections of laminate having respectively 30, 75 and 150 micrometres of ply thickness. The microstructure is more homogeneous in thin-ply composites than in thicker ply composites. This difference originates from the tow spreading procedure during the production of the prepregs. The 12K tows are spread until reaching the desired thickness for the plies, leading to wider pattern in thin-ply tapes than in thicker ones. This rectangular pattern is observable in intermediate and thick ply laminates.

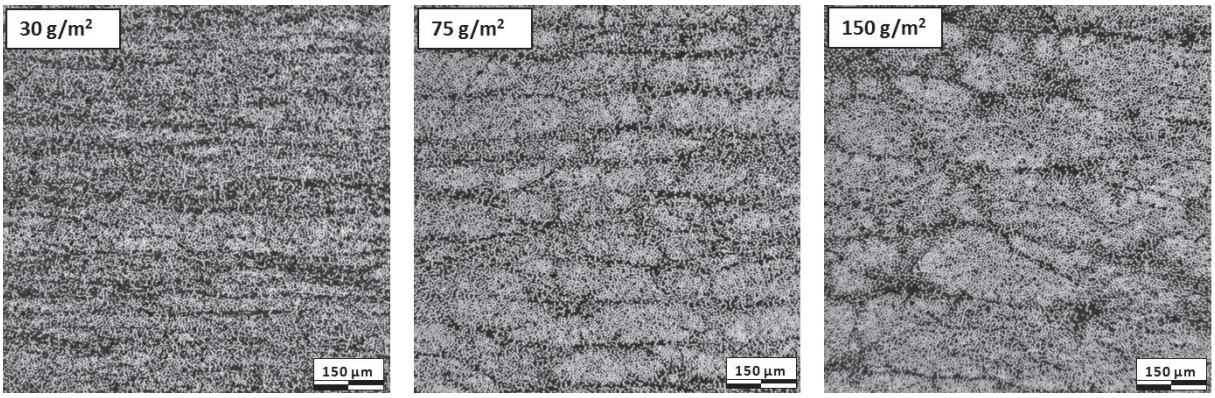

Figure 4 : Representative cross sections for different ply thicknesses

The heterogeneity of the microstructure is quantified by calculating the coarseness. This quantifier, which reflects the normalized standard deviation of the local fibre volume fraction (equation (2)), is sensitive to the windows size. However, whatever the window size, the coarseness is lower in thin-ply laminates than in standard ones, reflecting the visual observations (Figure 5 (a)). A higher heterogeneity of the microstructure leads to a higher probability of micro-cracking, which in turn results in a high probability to have a crack front split on different levels. This might traps fibres between both crack faces and eventually leads to the creation of large bundles of bridging fibres. This formation of bundles is observed in the cross sections, as illustrated in Figure 6. As the majority of the bridging fibres are not isolated, but clustered in bundles, this phenomenon is particularly important. As

a consequence of the microstructural heterogeneity, the number of bridging fibres is much higher in thick-ply laminates than in thin-ply laminates (Figure 5 (b)).

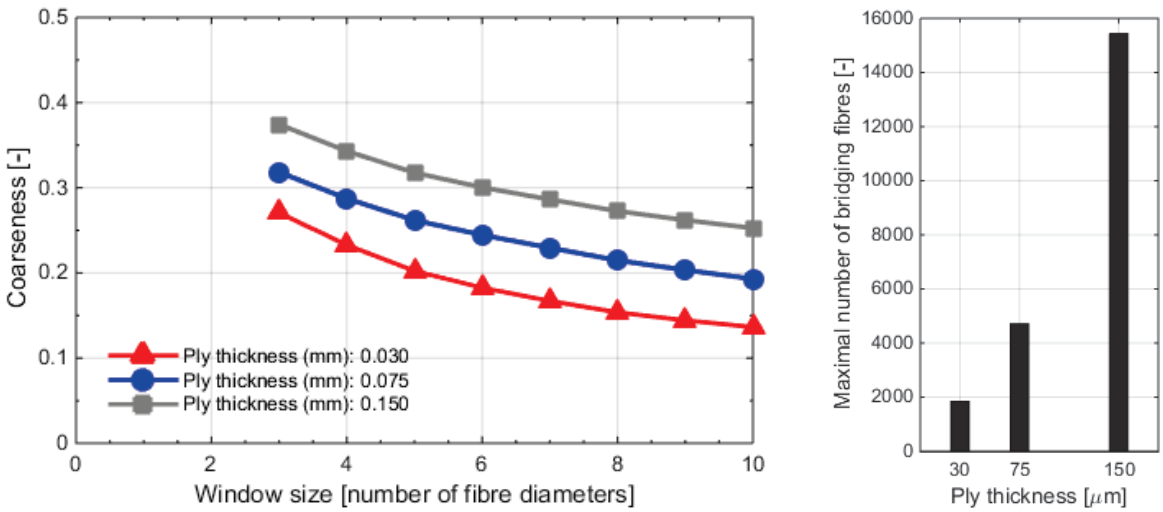

(a) (b)

Figure 5 : (a) Coarseness dependency on ply thickness; (b) Maximal number of bridging fibres for the different ply thicknesses

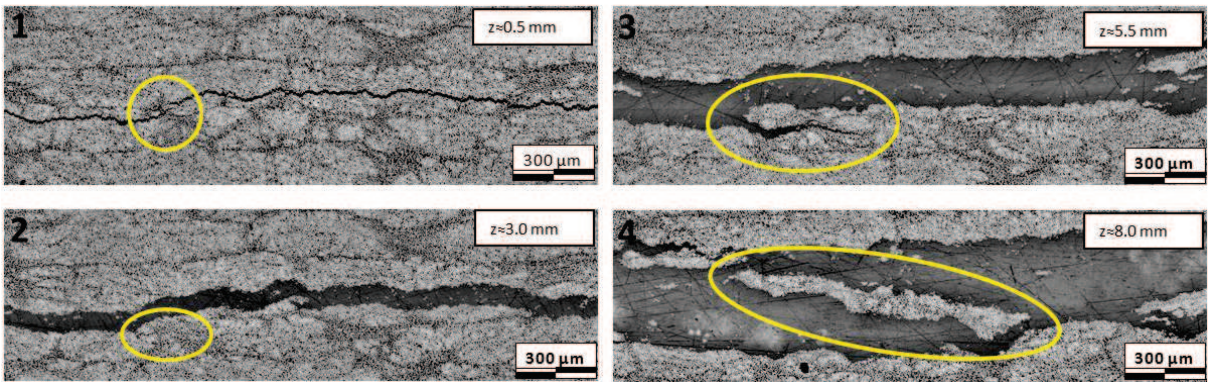

Figure 6 : Development of a bundle of bridging fibres

In summary, the ply thickness influences the homogeneity of the microstructure because of the tow spreading process involved in the production of the prepregs. The heterogeneity of the microstructure, reflected by the coarseness, allows the creation of large bundles of bridging fibres. Thus, the heterogeneity of the microstructure is correlated with the maximal number of bridging fibres counted in each specimen. Finally, the number of bridging fibres is directly related to the amount of bridging energy. This sequence, schematized in Figure 7, explains how the ply thickness is related to its effect on the steady-state ERR through the change of microstructure homogeneity.

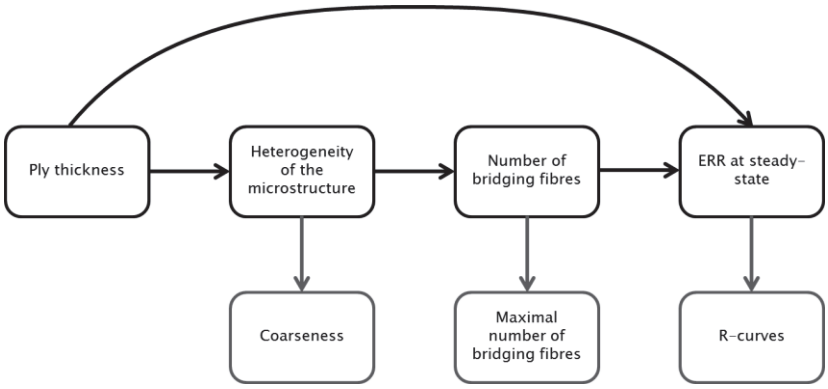

Figure 7 : Explanation of the cause of the ply thickness effect

4 CONCLUSION

A significant effect of the ply thickness on the mode I ERR in unidirectional DCB specimens is measured experimentally. While the ERR value at onset of crack propagation remains almost constant, the ERR at the plateau changes considerably. The steady-state energy is twice lower in thin-ply laminate than for the thicker-ply laminate.

This effect is attributed to differences of bridging fibre contribution and is originally caused by changes in the microstructure of the laminates. Cross sections observations show a fundamental change from a well homogenized microstructure in thin-ply laminate to a heterogeneous microstructure in thicker ply laminate. This difference, which is attributed to the tow spreading process involved in the prepregs production, is directly correlated with the amount of bridging fibres in the wake of the crack, and consequently to the energy associated to fibre bridging.

ACKNOWLEDGEMENTS

The authors thank North Thin Ply Technology, Lausanne, Switzerland for providing the material.

REFERENCES

[1] R. Amacher, J. Cugnoni, and J. Botsis, Thin ply composites: experimental characterization and modeling, *Proceeding of ICCM 19*, Montreal, 2013.

[2] S. Sihn, R. Y. Kim, K. Kawabe, and S. W. Tsai, Experimental studies of thin-ply laminated composites, *Composites Science and Technology*, 67, 2007, pp. 996-1008.

[3] L. Zengshan, G. Zhidong, H. Wei, and L. Debo, The effect of ply thickness on the damage mechanisms in notched composites, *Proceeding of ICCM 18*, Jeju, South Korea, 2011.

[4] E. Farmand-Ashtiani, J. Cugnoni and J. Botsis, Specimen thickness dependence of large scale fibre bridging in mode I interlaminar fracture of carbon epoxy composite, *International Journal of Solids and Structures*, 55, 2015, pp 58-65.

[5] B. D. Manshadi, A. P. Vassilopoulos and J. Botsis, A combined experimental/numerical study of the scaling effects on mode I delamination of GFRP, *Composites Science and Technology*, 83, 2013, pp 32-39.

[6] M. R. Wisnom, Size effects in the testing of fibre-composite materials, *Composites Science and Technology,* 59, 1999, pp. 1937-1957.

[7] ASTM, "Standard test method for mode I interlaminar fracture toughness of unidirectional fiber-reinforced polymer matrix composites," D5528-01, 2007.